INVESTIGATION OF THE MISCIBILITY OF PMMA/F2604 BLENDING SYSTEMS

Xi LI[1]*, Jian LI[2], Mi ZHOU[3], He ZHOU[4], Boliang WANG[5]*

Fluoropolymer (F2604) is a random copolymer of vinylidene fluoride and hexafluoropropene, with a molar ratio of 4:1. F2604 has good thermal stability, flame retardancy, excellent mechanical properties, and high chemical resistance to many types of oil, fuel, and concentrated acids. To evaluate the potential use of polymethyl methacrylate (PMMA)/F2604 composites in mixed explosives and propellants, the miscibility of PMMA/F2604 blending systems with F2604 mass ratios of 0%, 20%, 50%, and 80% is investigated through molecular dynamics (MD) simulations and differential scanning calorimetry (DSC) experiments. The miscibility between PMMA and F2604 is indicated based on the results of the blending ability and the difference in the obtained solubility parameters ($|\Delta\delta|$ = 0.99 <2.0 $(J/cm^3)^{1/2}$). The radial distribution function (g(r)) results show that the PMMA/2604 80/20 blend is more miscible than the 50/50 and 20/80 blends. The strong hydrogen bonding interactions between PMMA and F2604 favor the formation of miscible blends. Our results show a decrease in the glass transition temperature (T_g) of PMMA whenever F2604 is added, as observed through MD simulations. The T_g results agree well with the DSC experiments. The PMMA/F2604 80/20 blend exhibits better tensile strength and elongation at break compared to pure PMMA and the 50/50 and 20/80 blends.

Keywords: PMMA, F2604, miscibility, MD simulations, DSC

1. Introduction

Polymethyl methacrylate (PMMA), derived from the monomer MMA, is widely used in various civil applications. PMMA offers advantages such as aging resistance, favorable thermal stability, and chemical safety [1]. Recently, it has emerged as a coating material for polymer-bonded explosives (PBXs) and emulsion explosives [2-3]. However, PMMA is not considered an ideal material

[1] PhD Eng., Functional powder material laboratory of Bengbu City, Bengbu University, China, corresponding author, e-mail: lixivip89@163.com
[2] M.S., Nanjing University of Science and Technology, China, e-mail: lijian@njust.edu.cn
[3] PhD Eng., Functional powder material laboratory of Bengbu City, Bengbu University, China
[4] B.S., Anhui Xiangyuan Science and Technology Co., Ltd., Bengbu, Anhui, China.
[5] Prof., School of Chemical Engineering, Nanjing University of Science and Technology, China, corresponding author, e-mail: boliangwang@163.com
* Authors Xi Li and Jian Li contribute equally to our research

due to its relatively high glass transition temperature, brittleness, and low elongation at break [4-5].

In this context, to further improve the tensile properties of PMMA, various types of polymers have been selected. Tran et al. [6] attempted to enhance the mechanical properties of PMMA/polycarbonate (PC) blends with 20%, 50%, and 80% weight fractions of PC using one and multiple response optimization. The results showed that the improvement in tensile yield strength was negligible compared to the enhancement in impact strength after optimization. Kuleyin et al. [7] examined the fatigue behavior of PMMA/Acrylonitrile-Butadiene-Styrene (ABS) polymer blends with 40%, 50%, 60%, 70%, and 80% ABS, and found that the modulus of elasticity of the PMMA/ABS blend significantly decreased with the addition of ABS. A nonlinear change was concluded between the yield strength, tensile strength, and elasticity modulus of PMMA/ABS blend and the ABS composition in the blend structures. Rahman et al. [8] fabricated PMMA/ nanofibril-thermoplastic polyester elastomer (TPEE)-nanofibril composites containing 1, 3, 5, and 10 wt% of in situ fibrillated TPEE nanofibrils. The results suggested that when the addition of the TPEE nanofibrils increased, higher toughness of PMMA/TPEE composite and lower ultimate tensile stress were obtained than the neat PMMA. Notably, these additional materials could decrease the energy of mixed explosives. However, incorporating various energetic ingredients can enhance explosive energy. Fluororubber, a special energetic binder without energetic groups, has gained popularity in military applications due to its unique properties, including high density, low melting point, and plasticity [9-10]. Xia et al. prepared poly(vinylidene fluoride) (PVDF)/PMMA blend films using electrospinning methods with different PMMA concentrations ranging from 0 to 20 wt. % [11]. The tensile strength of electrospun PVDF/PMMA blends was enhanced compared to pure PVDF. There is a lack of information on the effect of higher PMMA content on the properties of PVDF. F2604 (FE2604-2), a typical fluororubber, has been successfully applied as a key material in many industrial fields [12-13]. Previous research has found that fluoroelastomer (FKM) can enhance the tensile strength and elongation at break of PVDF [14]. There is a promising prospect for combining PMMA and F2604 to achieve the desired comprehensive performance. However, the compatibility/miscibility and tensile properties for PMMA/F2604 binary systems has not been reported. This is a key aspect and should be carefully investigated before formulation design and technical applications.

The miscibility of polymer blends has been accurately predicted by molecular dynamics (MD) simulations [15]. The T_g parameter simulated by MD simulations can be commonly confirmed by differential scanning calorimetry (DSC) experiments. Also, the mechanical test was carried out to evaluate the influence of the F2604 content on the tensile modulus and elongations at break of PMMA/F2604 blends.

Therefore, in this work, the miscibility of PMMA/F2604 blends is explored using a combination of MD simulations and DSC. The results provide guidance for expanding the applications of PMMA and F2604 in mixed explosives.

2. Methods and details

Experimental procedure

F2604 was purchased from Inner Mongolia 3F Wanhao Fluorochemicals Co., Ltd. The fluororubber has molecular of $((CH_2CF_2)_x\text{-}(CF_2C(CF_3)F)_y)_n$ (x : y = 80:20) and the fluorine content about 66% by weight. Other properties of F2604 included a density of 1.82 g/cm^3, the Mooney viscosity of 71–80, tensile strength of more than 11 MPa (23 ± 2 °C) and tensile elongation of more than 150 % (23 ± 2 °C). PMMA was bought from Shanghai Aladdin Biochemical Technology Co., Ltd.

To investigate the glass transition temperature and tensile properties of the PMMA/F2604 polymer blends, total mass of 60 g PMMA/F2604 mixtures with mass ratio of 4:1, 1:1 and 1:4 was weighted and put into an internal mixer (QE-70C, Wuhan Qien Science & Technology Development Co, Ltd, China) with heating temperature about 140 ˚C for several minutes to be mixed, respectively. Once cooled to the temperature of the mold, The sample was taken out from the machine after the temperature after the temperature cooled down.

Mechanical characterization

The dumbbell specimens of pure PMMA and PMMA/F2604 blends after mixing were prepared through a hot press molding machine (R-3202, Wuhan Qien Science & Technology Development Co, Ltd, China). The conditions are as follows: hold pressure = 20 MPa bar, holding time = 5 minutes, and processing temperature = 140 ˚C. The solid tested samples were extracted from the mold when the temperature dropped to room temperature. Tensile behavior and elongation at break were measured refer to GB/T 1040-92 Type I specimen by a universal mechanical testing machine (AGS-X, Shimadzu, Japan) at a crosshead speed of 5 mm/min at 25℃. Six replicates were performed for each test.

Simulation procedure

A PMMA chain was constructed using the Visualizer module of Materials Studio with a repeat unit of methyl methacrylate. An F2604 chain was also built by Materials Studio software with a molecular structure of $((CH_2CF_2)_x\text{-}(CF_2C(CF_3)F)_y)_n$ (x:y = 4:1). The PMMA and F2604 structures were first minimized by a “Smart” algorithm for 5000 steps with “Ultra-fine” quality, where the convergence criteria were fixed at 0.01 kcal/(mol·nm) [16]. For PMMA, a 2000 ps MD simulation was then performed under the NVT ensemble at 298 K to obtain its optimal conformation [17]. The optimal structures of PMMA and F2604

were then put into the amorphous unit with densities of 1.18 g/cm^3 [18] and 1.82 g/cm^3, respectively, using the Amorphous cell (AC) module. The detailed parameters of all AC models are listed in Table 1. The AC models of PMMA, F2604 and PMMA/F2604 are depicted in Fig. 1.

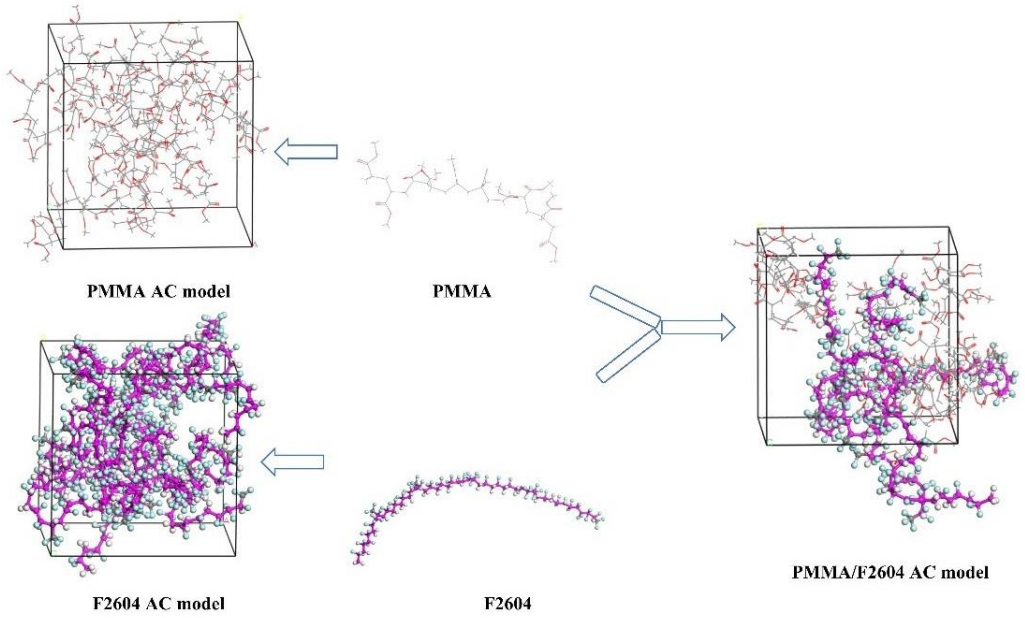

Fig 1. ACs of PMMA, F2604 and PMMA/F2604

For the constructed amorphous models, energy minimization procedures were also applied to eliminate unfavorable contacts. A MD simulation procedure with three steps was then conducted.

1. Annealing process: The systems were heated from 300 to 1000 K at intervals of 50 K and then cooled back at intervals of 50 K. The annealing cycle was 10. During the annealing treatment, a 10 ps MD simulation under 1 bar was applied at each temperature.

2. NVT–MD simulation: MD simulations were conducted via the NVT ensemble for 200 ps at 298 K. The first 150 ps and the final 50 ps were selected for equilibration and data collection, respectively, to analyze δ and g(r).

3. T_g. Following the 10-cycle annealing, 100 ps NVT and then 150 ps NPT MD simulations were performed for PMMA/F2604 systems at 520 K and then the systems were cooled down stepwise to 120–160 K at 20 K intervals. The final 50 ps trajectories were selected for analysis

In all MD simulations, the COMPASS force field was chosen and the Nosé thermostat was used to control the temperature [19-20]. A time step size of 1 fs was selected in this study. The Ewald and Atom-Based truncation methods

were employed to evaluate the Coulomb and van der Waals long-range nonbonding interactions. The cut-off radii for spline width, nonbonding interactions and buffer width were 0.10, 0.95 and 0.05 nm, respectively [21].

Table 1

Parameters for PMMA/F2604 binary systems

PMMA/F2604	initial density (g/cm^3)	atom number	mass ratio
100/0	1.18	1220	
80/20	1.3125	1265	0.793/0.207
50/50	1.4987	1335	0.498/0.502
20/80	1.6901	1201	0.203/0.797
0/100	1.82	1169	

3. Results and discussions

3.1 Blending ability and Solubility Parameters

The Blends module was used to screen the miscibility of polymer blends. The miscibility behaviors between PMMA and F2604 were analyzed through the Blends module with the COMPASS force field. During the Blends calculation, the PMMA and F2604 macromolecules were selected as the base and as the screen, respectively. The energy distribution results from the Blends module are plotted in Fig. 2. A miscible system can be regarded when the energy distributions are similar for the base-screen (E_{bs}), base-base (E_{bb}) and screen-screen (E_{ss}) [22]. As illustrated in Fig. 2, there is a single peak for the PMMA/F2604 blend. PMMA/F2604 blends show fine miscibility resulting from the similar energy distributions.

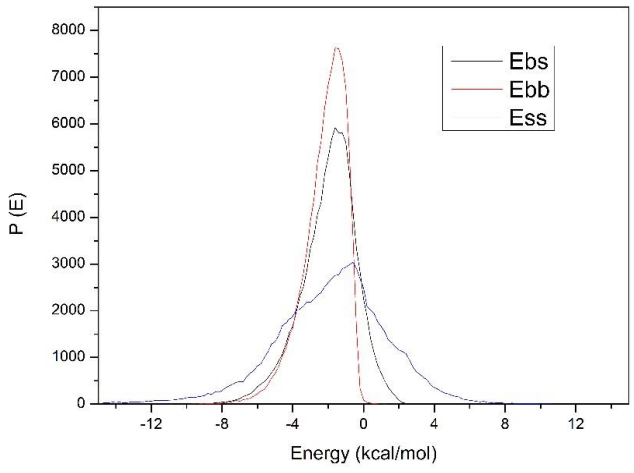

Fig. 2. Energy distribution of the PMMA matrix blended with F2604

The δ parameter has widespread use in investigating the physical compatibility of materials [23]. This is directly related to the cohesive energy density (CED) and is mathematically evaluated by Equation (1). To further compare the miscibility of the PMMA/F2604 blends, the solubility parameters of PMMA and F2604 were calculated, as shown in Table 2.

$$\delta = \sqrt{\mathrm{CED}} \tag{1}$$

Empirically, if the solubility parameter difference ($|\Delta\delta|$) between two polymers A and B is not more than 2.0 $(J/cm^3)^{1/2}$, then A and B are regarded miscible, otherwise an immiscible result is obtained [24] As displayed in Table 2, the calculated δ of PMMA and F2604 are in accordance with the reported results from the literature, ensuring the reliability of simulated results. The calculated $|\Delta\delta|$ value for PMMA/F2604 is 0.96 $(J/cm^3)^{0.5}$, meaning that PMMA and F2604 are miscible. The result is prior to the formation of a miscible system and not likely to stratification. Meanwhile, when the δ vdw and δ elec values were compared for PMMA and F2604, respectively, the values of δ vdw were found to be always larger than δ elec. The results indicated that Van der Waals force has a key effect on the molecular interaction between PMMA chains and F2604 chains.

Considering the above results of blending ability and solubility parameters, PMMA demonstrates compatibility with F2604, and the reasons may be the fact that the high fluorine content of F2604 results in stronger electrostatic interaction and higher density between F2604 and PMMA, which may strengthen the intermolecular interaction of the F2604/PMMA blends, resulting in compatibility between F2604 and PMMA.

Table 2

Solubility parameters of PMMA/F2604 blends (δ, $(J/cm^3)^{0.5}$)

Species	δ	δ_{vdw}	δ_{elec}	$\lvert\Delta\delta\rvert$
PMMA	18.90 (18.55) [25]	16.72	6.16	0.96
F2604	17.94 （17–25） 26]	13.51	10.53	

3.2 g(r)

The *g*(r) function can embody the characteristics of the microstructure and ascertain the degree of miscibility of polymer blends [27], as defined in Equation (2):

$$g_{\mathrm{AB}}(r) = \frac{1}{\rho_{\mathrm{AB}} 4\pi r^2} = \frac{\sum_{t=1}^{K}\sum_{j=1}^{N_{AB}} \Delta N_{\mathrm{AB}}(r \to r+\delta r)}{N_{\mathrm{AB}} \times K} \tag{2}$$

where N_{AB} represents the total number of atoms of A and B in the system, K and δ_r are the number of time steps and the distance interval, respectively. ΔN_{AB} is related to the number of A (or B) atoms between r to $r+\delta r$ around an B (or A) atom and ρ_{AB} is the bulk density. In general, a blending system is considered compatible as a result of the intermolecular $g(r)$ of AB is higher than that of AA and BB [28]. The g(r) function can provide more detailed prediction of the miscibility of the polymer blends than blend analysis and solubility parameters.

Fig. 3a illustrates the $g_{C\text{-}C}^{\ intra}(r)$ of PMMA in the pure PMMA and PMMA/F2604 blends. For the PMMA chain, the highest and the second peak, indicating bond connectivity, are at 0.37 and 0.26 nm, respectively. When the PMMA content decreases from 100% to 20%, the peaks become higher primarily due to the reduced bulk density of PMMA in Equation (2).

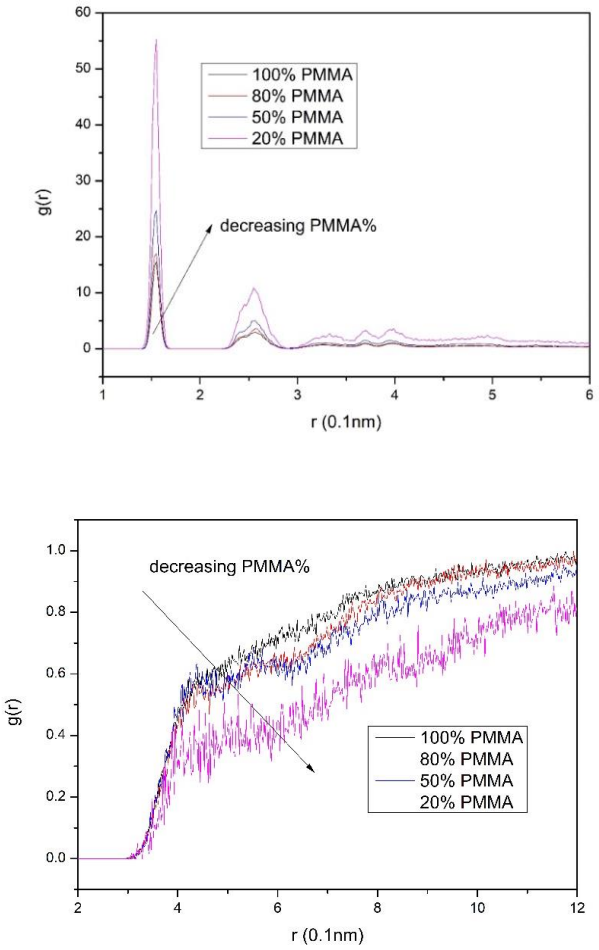

(a). $g_{C\text{-}C}^{\ intra}(r)$ of PMMA at 298 K (b) $g_{C\text{-}C}^{\ inter}(r)$ of PMMA at 298 K

Fig. 3. $g_{C\text{-}C}^{\ intra}(r)$ and $g_{C\text{-}C}^{\ inter}(r)$of PMMA at 298 K

The $g(r)$ could suggest the interactions of PMMA and F2604 chains. Fig. 3b shows the $g_{C\text{-}C}^{\ inter}(r)$ of PMMA chains in the pure PMMA and PMMA/F2604 blending systems. There exists a distinct peak of ~4.2 Å for pure PMMA. The value of g(r) decreases with decreasing PMMA content. This result indicates the weaker adjacent interactions between different PMMA chains with the addition of F2604. The $g_{C\text{-}C}^{\ inter}(r)$ of PMMA or F2604 chains themselves are also calculated in PMMA/F2604 blending systems.

Fig. 4 shows that the $g(r)$ of PMMA/F2604 is higher than that of PMMA-PMMA and F2604-F2604 in PMMA/F2604 blend with PMMA content of 80%, and partly higher in the blends with PMMA content of 50% and 20%. This means that the F2604 polymer has more degree of contact with the PMMA for PMMA/F2604 80/20 blends than others. These $g(r)$ results suggest that PMMA/F2604 blends show good miscibility when PMMA content is rich.

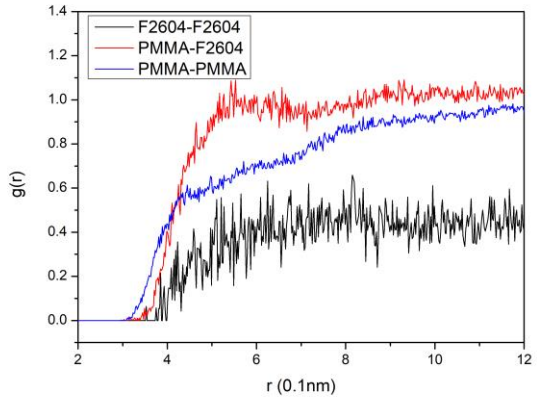

(a) PMMA/F2604 80/20

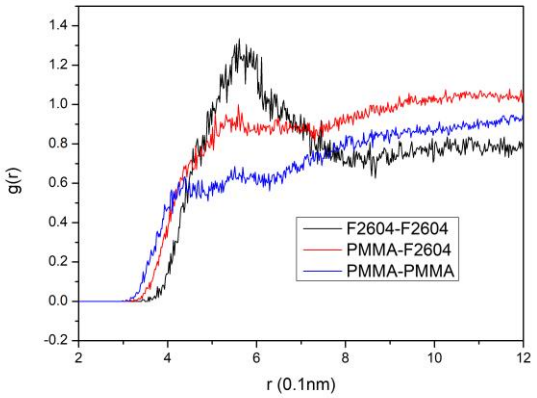

(b) PMMA/F2604 50/50

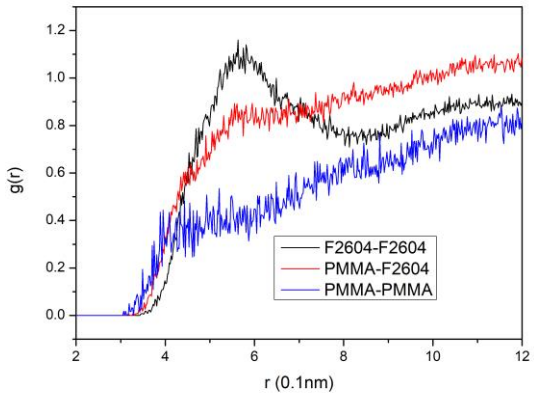

(c) PMMA/F2604 20/80

Fig. 4. $g_{C\text{-}C}^{inter}(r)$ of PMMA/F2604 blends

Exploring the intermolecular interactions between the molecular chains of PMMA/F2604 blends is helpful to understand the miscibility mechanism. Hydrogen bonds dominated the interactions of various molecular chains in polymer systems [29]. To verify the hydrogen bond interaction in PMMA/F2604 blends, the O atoms of the carbonyl groups (−C=O) in PMMA were signed as O(C=O), the H atoms in F2604 and PMMA were marked as H_{F2604} and H_{PMMA}, respectively. Fig. 5 shows the *g(r)s* of O(C=O)~H and O(C=O)~H_{PMMA} atoms in PMMA/F2604 blends. Generally, the distances of lower than 0.35nm belong to chemical bond and hydrogen bonding, and the value above 0.35 nm is dominated by vdW forces, respectively [30]. Obviously, from Fig.5a, the obvious peak *g*(*r*)*s* of O(C=O)~H of different PMMA/F2604 blends are all less than 0.35nm, indicating the formation of strong hydrogen bond and the vdW forces. In addition, weak peak *g(r)s* of O(C=O)~H_{PMMA} show a small part of them have interaction by hydrogen bonds but strong interaction of vdW forces, as shown in Fig.5b. Based on the above analysis of intermolecular interactions, we can find that the hydrogen bond is the mainly interactions of functional groups (−C=O) of PMMA chains in PMMA/F2604 blend systems interact with H atoms of F2604. Hydrogen bond can also be formed between the polar functional groups and surrounding H atoms in the blends, as shown in Fig 6. The result reveals a good stability miscibility result for the formed PMMA/F2604 blends.

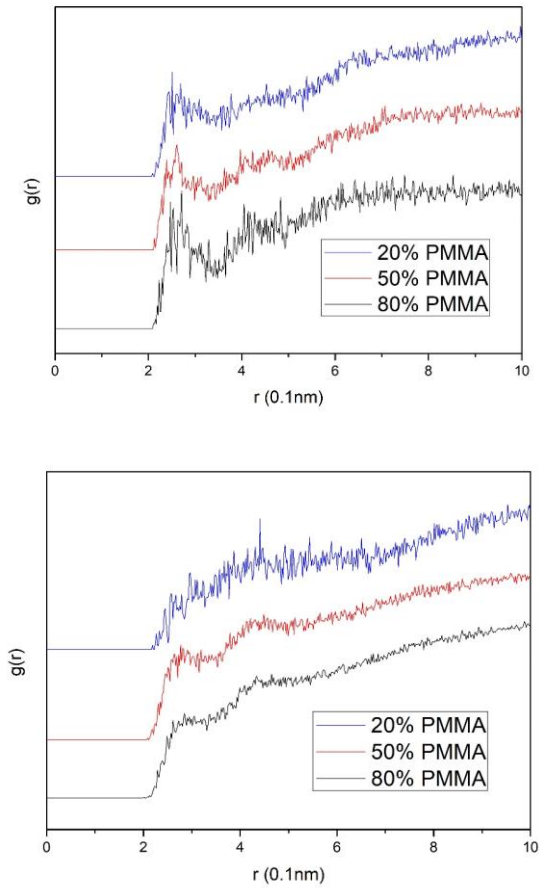

(a) $g(r)$ of O (-C=O) in PMMA~ H in F2604 (b) $g(r)$ of O (-C=O)~H_{PMMA}

Fig. 5. $g(r)$ of possible hydrogen bond of PMMA/F2604 blends

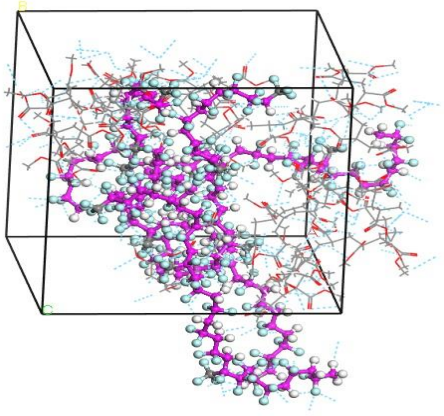

Fig. 6. Hydrogen bonding formation (blue dotted bonds) of PMMA/F2604 blends with 50% PMMA

3.3 T_g

T_g is a key property of polymers as it can determine the scope of application [31]. The parameter can also be applied to verify the miscibility of polymers. The T_g values are often calculated based on Fox-Flory's free volume theory. T_g values of pure PMMA and PMMA/F2604 blends were obtained by computing the turning point of density-temperature profiles and the results are plotted in Fig. 7 and Table 3. From Fig.7, it is found that the density of PMMA/F2604 systems decrease with the increase of temperature. Obviously, the notable change can be found in the slop of each curve, and then the T_g of PMMA/F2604 blends can be computed.

To obtain the experimental T_g values of pure PMMA (purchased from aladdin-e.com) and PMMA/F2604 blends, the DSC test (see Fig. 8) was performed on a PerkinElmer Thermal Analysis under the temperature range from -30 to 180 ℃ and a heating rate of 10 ℃/min. Table 3 shows the T_g results of calculation and DSC experiment. From simulation results, the simulated T_g values of pure PMMA, 80PMMA/20F2604, 50PMMA/50F2604 and 20PMMA/80F2604 blends are 366, 330, 311 and 296 K, respectively. While for the DSC results, these values are 350, 341, 303 and 286 K, respectively. The gap of $|\Delta T|$ between simulated and experimental results are 16, 11, 8 and 10 K for pure PMMA and PMMA/F2604 blends, showing acceptable agreement. In addition, as shown in Table 3, the T_g values of our simulations and experiments of pure PMMA and F2604 are consistent with those of other works.

PMMA is a high T_g material, while F2604 is a low T_g material with better extensibility. The mobility of the PMMA chains increases with the addition of F2604, resulting in average mobility for the PMMA/F2604 blends. Consequently, the interactions between PMMA molecular chains are reduced by F2604. The T_g of PMMA/F2604 blends gradually decreases with the increase in F2604 content. Therefore, the addition of F2604 to PMMA can effectively reduce rigidity and increase plasticity.

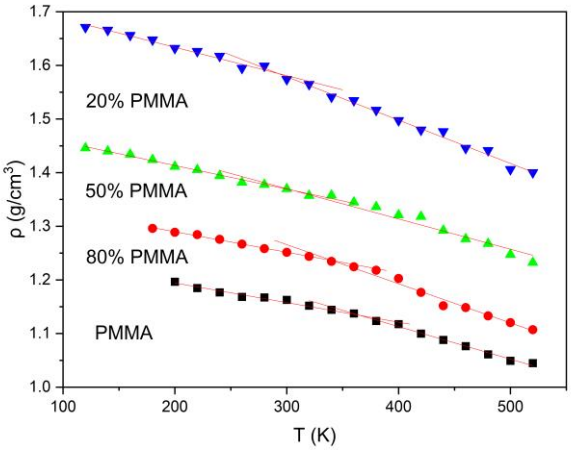

Fig. 7. Density-Temperature curves of PMMA/F2604 blends

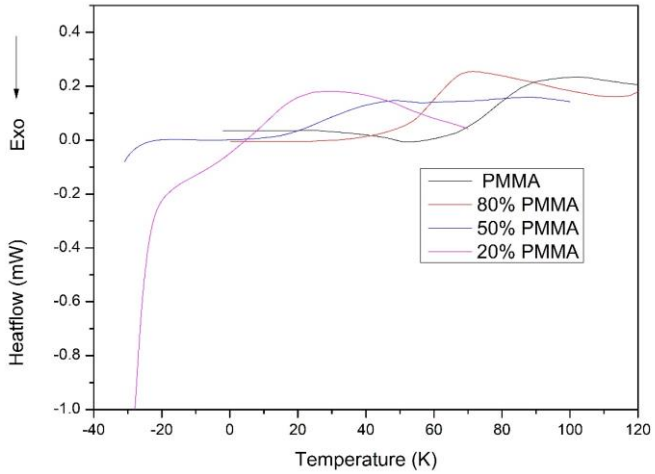

Fig. 8. DSC records of PMMA and PMMA/F2604 mixtures

Table 3

T_g value from simulations and experiments (K)

Sample	Simulation	Experiment
PMMA	366 (355 [32], 388.9 [33])	350 (351 [34], 370 [35])
80% PMMA	330	341
50% PMMA	311	303
20% PMMA	296	286

3.4 Tensile properties

The tensile strength and elongation at break values for the blend samples prepared with and without F2604 are displayed in Table 4 and Fig. 9. As can be seen from Table 4 and Fig. 9, the blend samples for tensile strength exhibit a slight increase first then an obvious decrease with the increasing F2604 content. The blend sample with 20 wt. % F2604 exhibits the maximum tensile strength and about 38% higher than that of pure PMMA, which could be the indication of good compatibility of the blend in tested PMMA/F2604 composites. The elongation at break values for 20% PMMA and 80% PMMA blend are about 73% and 46% higher than pure PMMA, respectively. For 20% PMMA sample, 102 times enhanced in elongation at the break when compared to pure PMMA. These results show that unlike the brittleness of pure PMMA, the high flexibility and mechanical property can be enhanced by the addition of F2604.

Table 4

Tensile strength (MPa) and elongation at break (%) for tested samples

Sample	Tensile strength	Elongation at break
PMMA	37.6 ± 5.5	5.6 ± 0.4
80% PMMA	51.9 ± 3.9	9.7 ±1.1
50% PMMA	38.3 ± 2.0	8.2 ± 0.4
20% PMMA	15.7 ± 1.9	579.5 ± 50.8

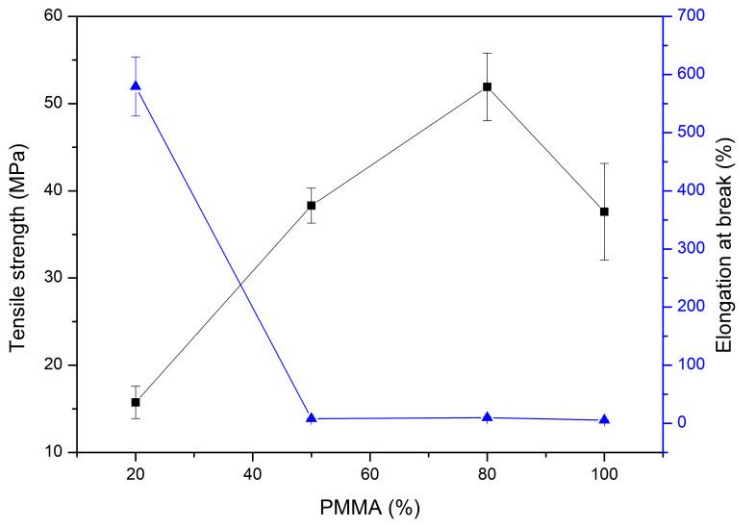

Fig. 9. Tensile strength and elongation at break for pure PMMA and PMMA/F2604 blend samples

4. Conclusions

The miscibility of PMMA/F2604 blends is predicted through molecular dynamics simulations. The blending ability and solubility parameter results ($|\Delta\delta|$ = 0.99 <2.0(J/cm^3)$^{1/2}$) show that the PMMA and F2604 are miscible. The g(r) results indicate that strong hydrogen bond formation between PMMA and F2604 favors the formation of a miscible blend. The PMMA/F2604 80/20 blend is more miscible than the 50/50 and 20/80 blends. The strong hydrogen bonding interactions between PMMA and F2604 favor the formation of a miscible blend. Based on the density-temperature curves, the simulated T_g values of PMMA/F2604 blending systems decrease with the addition of F2604, and the results show good agreement with the DSC experiments. The PMMA/F2604 80/20 blend exhibits better tensile strength and elongation at break than the 50/50 and 20/80 mixtures according to the mechanical tests. These results are useful for expanding the application of PMMA/F2604 mixtures and other blends.

Acknowledgements

The project is sponsored by the Natural Science Research Projects of Universities of Anhui Province (No. 2023AH052944, and 2022AH051918), the applied research projects of Bengbu University (2024YYX48QD, 2024YYX36pj), the Biobased Materials Research Team (BBXYKYTDxjZD03), and the Project of Industry-University Research Cooperation (No. 00013356, and 00013351). We thank International Science Editing (http://www.internationalscienceediting.com) for editing this manuscript.

R E F E R E N C E S

[1] Jia, X.L., Xu, L.J., Hu, Y.Y., Li, C., Geng, X.H., Guo, H.Y., Liu, X.W., Tan, Y.X., and Wang, J.Y. Preparation of Agglomeration-free Composite Energetic Microspheres Taking PMMA-PVA with Honeycomb Structure as Template via the Molecular Collaborative Self-assembly. J. Energ. Mater., vol. 39, no. 2, pp.182-196, 2021.

[2] Yao, Y.L., Cheng, Y.F., Liu, R., Hu, F. F., Zhang, Q. W., Xia, Y., and Chen, Y. Effects of Micro-Encapsulation Treatment on the Thermal Safety of High Energy Emulsion Explosives with Boron Powders. Propell. Explos. Pyrot., vol. 46, no. 3, pp. 389-397, 2021.

[3] Li, J., Jin, S.H., Lan, G.C., Chen, K., Liu, W., Zhang, X., Chen, S.S. and Li, L. J. A Molecular Dynamics Study and Detonation Parameters Calculation of 5, 5'-dinitramino-3, 3'-bi [1, 2, 4-triazolate] carbohydrazide salt (CBNT) and Its PBXs. J. Energ. Mater., vol. 38, no. 3, pp. 283-294, 2020.

[4] Zhang, C., Liu, X.H., Liu, H., Wang, Y.M., Guo, Z.H., and Liu, C.T. Multi-walled Carbon Nanotube in a Miscible PEO/PMMA Blend: Thermal and Rheological Behavior. Polym. Test., vol, 75, pp. 367-372, 2019.

[5] Torabi A. R., Saboori B., Mohammadian S. K., and Ayatollahi, M. R. Brittle Failure of PMMA in the Presence of Blunt V-notches under Combined Tension-tear Loading: Experiments and Stress-based Theories. Polym Test, 2018, vol, 72, pp. 94-109.
[6] Tran MS., Hoang VT, and Park JM. The One/multi-objective Optimization for Tensile Yield and Impact Strength Responses of Optical PC/PMMA Blends. International Journal of Precision Engineering and Manufacturing, 2022, vol, 23, no, 4, pp. 405-419.
[7] Kuleyin H, Gümrük R, and Çalişkan S. The Effect of ABS Fraction on the Fatigue Behavior of PMMA/ABS Polymer Blends. Mater Today Commun, 2022, vol. 33, pp. 104139.
[8] Rahman S. S., Mahmud M. B., Monfared A. R., Lee P. C., and Park C. B. Achieving Outstanding Toughness of PMMA while Retaining its Strength, Stiffness, and Transparency Using in situ Developed TPEE Nanofibrils. Composites Science and Technology, 2023. vol .236, pp. 109994.
[9] Wang Y.Z., Bi L.Y., Zhang H. J., Zhu, X.T., Liu, G.Y., Qiu, G. X., and Liu, S.S. Predictive Power in Oil Resistance of Fluororubber and Fluorosilicone Rubbers Based on Three-dimensional Solubility Parameter Theory. Polym. Test., vol. 5, pp. 380-386., 2019.
[10] Tao, J., Wang, X.F. Molecular Dynamics Dimulation for Fluoropolymers Applied in ε-CL-20-based Explosive. J. Adhes. sci. Technol., vol. 31, no. 3, pp. 250-260, 2017.
[11] Xia J, Zheng Z, Guo Y. Mechanically and electrically robust, electro-spun PVDF/PMMA blend films for durable triboelectric nanogenerators[J]. Composites Part A-Appl S., 2022, vol. 157, pp: 106914.
[12] Yao, J., Li, B., Xie, L. F., and Peng, J.H. Electrospray Preparation and Properties of RDX/F2604 Composites. J. Energ. Mater., vol. 36, no. 2, pp. 223-235, 2018.
[13] Xu, Z., Zhang, Y., Li, A., Wang, J., Wang, G., and He, Q. Research progress on compounding agent and mechanical test method of fluororubber. J Appl Polym Sci, vol.138, no. 36, pp 50913,2021.
[14] Zhou, Z., Zhang, X., Zhang, W., Li, J., and Lu, C. Microstructure and properties of solvent-resistant fluorine-contained thermoplastic vulcanizates prepared through dynamic vulcanization. Mater Design, 2013, vol. 51, pp. 658-664.
[15] Li, J., Jin, S. H., Lan, G. C., Xu, Z. S., Wang, L. T., Wang, N., and Li, L. J. Research on the Glass Transition Temperature and Mechanical Properties of poly (vinyl chloride)/dioctyl phthalate (PVC/DOP) Blends by Molecular Dynamics Simulations. Chinese. J. Polym. Sci., vol. 37, no. 8, pp. 834-840, 2019.
[16] Yang, J.Q., Zhang, X.L., Gao, P., Gong, X.D., and Wang, G.X. Molecular Dynamics and Dissipative Particle Dynamics Simulations of the Miscibility and Mechanical Properties of GAP/DIANP Blending Systems. RSC adv., vol. 4, no. 79, pp.41934-41941, 2014.
[17] Li., J., Jin, S.H., Lan, G.C., Chen, S.S., and Li, L.J. Molecular Dynamics Simulations on Miscibility, Glass Transition Temperature and Mechanical Properties of PMMA/DBP Binary System. J. Mol.Graph. Model., vol. 84, pp. 182-188, 2018.
[18] Hao, X., Kaschta, J., Liu, X., Pan, Y., and Schubert, D.W. Entanglement Network Formed in Miscible PLA/PMMA Blends and its Role in Rheological and Thermo-mechanical Properties of the Blends. Polymer., vol, 80, pp, 38-45, 2015.
[19] Okada, O., Oka, K., Kuwajima, S., Toyoda, S., and Tanabe, K. Molecular Simulation of an Amorphous Poly (methyl methacrylate)–poly (tetrafluoroethylene) Interface. Comput. Theor. Polymer. Sci., vol. 10, no. 3-4, pp. 371-381, 2000.
[20] Sun, H. COMPASS: Sn ab initio Force-field Optimized for Condensed-phase Applications Overview with Details on Alkane and Benzene Compounds. J. Phys. Chem. B., vol. 102, no. 38, pp. 7338-7364, 1998.
[21] Yang, J.Q., Gong, X.D., Wang, G.X. Compatibility and Mechanical Properties of BAMO–AMMO/DIANP Composites: A Molecular Dynamics Simulation. Comp. Mater. Sci., vol. 102, pp.1-6, 2015.

[22] Zhao, Y., Zhang, X.H., Zhang, W., Xu, H.J., Xie, W.X., Du, J.J., and Liu, Y.Z. Simulation and Experimental on the Solvation Interaction between the GAP Matrix and Insensitive Energetic Plasticizers in Solid Propellants. J. Phys. Chem. A., vol. 120, no.5, pp.765-770, 2016.

[23] Lan, G. C., Jin, S.H., Li, J., Wang, J.Y., Lu, Z.Y., Wu, N.N., and Li, L.J. Miscibility, Glass Transition Temperature and Mechanical Properties of NC/DBP Binary Systems by Molecular Dynamics. Propell. Explos. Pyrot., vol. 43, no. 6, pp. 559-567, 2018.

[24] Forster, A., Hempenstall, J., Tucker, I., and Rades, T. Selection of Excipients for Melt Extrusion with two Poorly Water-soluble Drugs by Solubility Parameter Calculation and Thermal Analysis. Int. J. Pharmaceut., vol. 226, no. 1-2, pp. 147-161, 2001.

[25] Chen, S., Xu, C.B., Ma, M., Shi, Y.Q., He, H. W., Yuan, K.Y., Xu, R.Q., and Wang, X. Application of Solubility Parameters in the Preparation of PMMA with Permanent Antistatic, High toughness, and Excellent Optical Properties. Polym. Advan. Technol., vol. 32, no. 9, pp. 3750-3758, 2021.

[26] Wang, H.Y., Rehwoldt, M., Kline, D. J., Wu, T., Wang, P., and Zachariah, M. R. Comparison Study of the Ignition and Combustion Characteristics of Directly-written Al/PVDF, Al/Viton and Al/THV Composites. Combus. Flame., vol. 201, pp. 181-186, 2019.

[27] Takhulee, A., Takahashi, Y., and Vao-soongnern, V. Molecular Simulation and Experimental Studies of the Miscibility of Polylactic acid/polyethylene glycol Blends. J. Polym. Res., vol. 24, no. 1, pp. 1-10, 2017.

[28] Clancy, T. C., Pütz, M., Weinhold, J. D., Curro, J. G., and Mattice, W. L. Mixing of Isotactic and Syndiotactic Polypropylenes in the Melt. Macromolecules., vol. 33, no. 25, pp. 9452-9463, 2000.

[29] Wei Q, Wang Y, Che Y, et al. Molecular mechanisms in compatibility and mechanical properties of Polyacrylamide/Polyvinyl alcohol blends. Journal of the Mechanical Behavior of Biomedical Materials, 2017, 65: 565-573.

[30] Wei Q, Wang Y, Chai W, et al. Effects of composition ratio on the properties of poly (vinyl alcohol)/poly (acrylic acid) blend membrane: A molecular dynamics simulation study. Materials & Design, 2016, 89: 848-855.

[31] Bertinetto, C., Duce, C., Micheli, A., Solaro, R., Starita, A., and Tiné, M. R. Prediction of the Glass Transition Temperature of (meth) acrylic Polymers Containing Phenyl Groups by Recursive Neural Network. Polymer., vol. 48, no. 24, pp. 7121-7129, 2007.

[32] Bouzid, L., Hiadsi, S., Bensaid, M. O., and Foudad, F. Z. Molecular Dynamics Simulation Studies of the Miscibility and Thermal Properties of PMMA/PS Polymer Blend. Chinese. J. Phys., vol. 56, no. 6, pp. 3012-3019, 2018.

[33] Berrahou, N., Mokaddem, A., Doumi, B., Hiadsi, S., Beldjoudi, N., and Boutaous, A. Investigation by Molecular Dynamics Simulation of the Glass Transition Temperature and Elastic Properties of Amorphous Polymers PMMA, PMAAM and PMMA co PMAAM copolymers. Polym.Bull., vol. 73, no. 11, pp. 3007-3017, 2016.

[34] Mathur, V., and Sharma, K. Thermal Response of Polystyrene/poly Methyl methacrylate (PS/PMMA) Polymeric Blends. Heat. Mass. Transfer., vol. 52, no. 12, pp. 2901-2911, 2016.

[35] Lang, L., Shi-Jun, L., Guo-Dong, Z., Xing-Ping, Z., Dian-Zeng, J., and Xiao-Lin, X. Microstructure and Photochromic Behavior of PMMA-dispersed Spiropyran Films. Chem. J. Chinese. U., vol. 31, no. 9, pp. 1868-1873, 2010.